



Eqs. (2) reduce to a more familiar form<sup>6</sup>

$$\Delta W^{J,|M|} = -\frac{E^2}{2} \left[ \alpha_0^J + \alpha_2^J \frac{3M^2 - J(J+1)}{J(2J-1)} \right]. \quad (4)$$

In this limit, the overall Stark shifts of components hav-

ing a given  $J$  are governed by a scalar polarizability  $\alpha_0^J$ , while the splitting according to the value of  $M$  is governed by a tensor polarizability  $\alpha_2^J$ .

The theory of the quadratic Stark effect also provides expressions for the polarizabilities. For  ${}^2D$  states of alkali-metal atoms these may be written as

$$\alpha_0^{5/2} = e^2 \sum_{n'} \frac{4}{15} \frac{|R_{n'P}^{nD}|^2}{W^0 - W_{n'P3/2}^0} + \frac{2}{5} \frac{|R_{n'F}^{nD}|^2}{W^0 - W_{n'F}^0}, \quad (5a)$$

$$\alpha_0^{3/2} = e^2 \sum_{n'} \frac{2}{45} |R_{n'P}^{nD}|^2 \left[ \frac{1}{W^0 - W_{n'P3/2}^0} + \frac{5}{W^0 - W_{n'P1/2}^0} \right] + \frac{2}{5} |R_{n'F}^{nD}|^2 (W^0 - W_{n'F}^0)^{-1}, \quad (5b)$$

$$\alpha_2^{5/2} = -e^2 \sum_{n'} \frac{4}{15} \frac{|R_{n'P}^{nD}|^2}{W^0 - W_{n'P3/2}^0} + \frac{2}{35} \frac{|R_{n'F}^{nD}|^2}{W^0 - W_{n'F}^0}, \quad (5c)$$

$$\alpha_2^{3/2} = -e^2 \sum_{n'} \frac{2}{45} |R_{n'P}^{nD}|^2 \left[ \frac{-8/225}{W^0 - W_{n'P3/2}^0} + \frac{2/9}{W^0 - W_{n'P1/2}^0} \right] + \frac{2}{25} |R_{n'F}^{nD}|^2 (W^0 - W_{n'F}^0)^{-1}. \quad (5d)$$

Here  $R_{n'L}^{n'L'}$  are radial integrals between states having principal and angular momentum quantum numbers  $n, L$  and  $n', L'$ , while  $W^0$  and  $W_{n'L'}^0$  are zero-field energies of the  ${}^2D$  state and intermediate states, respectively. Only intermediate states (such as  $P$  and  $F$ ), which are dipole-connected with a  ${}^2D$  state contribute to its polarizability. Furthermore, in Rb, more than 99% of the polarizability (scalar or tensor) of a given  ${}^2D$  state is contributed by neighboring intermediate states. Hence, for a given  $n^2D$  state, the summations of Eqs. (5) (which in principle are taken over all allowed discrete and continuum intermediate states) can be truncated to include only the  $(n+1)P$ ,  $(n+2)P$ ,  $(n-1)F$ , and  $(n-2)F$  states, with a decrease of only  $\sim 1\%$  in the accuracies of calculated polarizabilities.

### III. EXPERIMENT

Spectra of the transitions  $n^2D_{3/2,5/2} \leftarrow 5^2S_{F=3}$  were obtained by inducing Doppler-free two-photon absorptions in Rb vapor at 5 mTorr pressure. Atoms having absorbed two photons from counter-propagating laser beams were ionized by thermal collisions, and detected with a thermionic diode detector. The laser light was modulated by a 12-Hz chopper, enabling synchronous detection of the resulting ions.

Two Pyrex cells containing ion detectors and Rb vapor were used. The Stark cell also housed a parallel-plate Stark electrode assembly,<sup>1</sup> and the reference cell contained a small Faraday cage attached to the detector which ensured zero fields for excited atoms and ions. In the Stark cell, electric fields as large as  $10^3$  V/cm and uniform to within 0.03% were produced without an electric discharge. Since the Stark electrode spacing was accurately known<sup>1</sup> [1.02445(8) cm] electric fields could be determined with relative accuracies of 0.1 to 0.4% by measuring applied voltages with a calibrated voltmeter.

The radiation from an Ar<sup>+</sup> laser was used to pump a frequency stabilized ( $\sim 2$  MHz jitter) and tunable R6G dye laser. Its output beam of 30–300 mW was focused and retro-reflected into both the Stark and reference cells to permit Doppler-free two-photon absorption, with a portion being directed into a 1.2-m confocal etalon. As the dye laser frequency was tuned through a two-photon resonance in Rb, signals from the Stark and reference cells were sensed with lock-in amplifiers and recorded on a three-pen chart recorder, along with transmission maxima from the etalon. In this way, Stark shifts and splittings of  ${}^2D$  lines were recorded, and could be measured within 2 MHz for any value of the electric field produced in the Stark cell.

### IV. OBSERVED SPECTRA AND STARK SHIFT MEASUREMENTS

A typical chart record illustrating the Stark shifts and splittings is shown in Fig. 1. Here, the  ${}^2D$  fine-structure

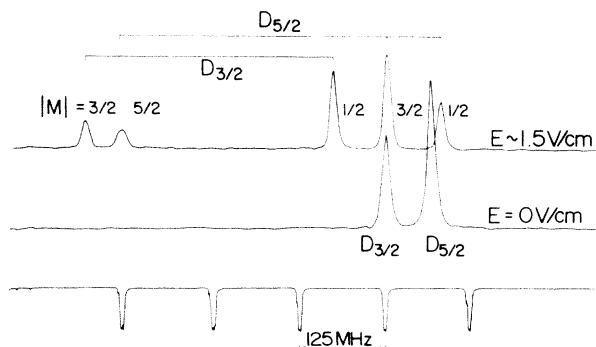


FIG. 1. Spectra of the  $50^2D_{3/2,5/2} \leftarrow 5^2S_{F=3}$  transition in  ${}^{85}\text{Rb}$ . The two fine-structure components at  $E=0$  (middle trace) are split into five components by the electric field (top trace). The etalon fringes (bottom trace) provide a frequency scale.

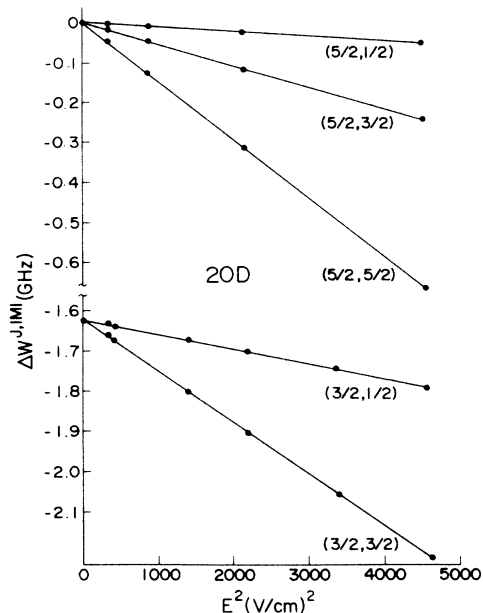


FIG. 2. Low-field Stark shifts of components  $J, |M|$  for the transition  $20^2D_{3/2,5/2} \leftarrow 5^2S_{F=3}$  plotted against  $E^2$ .

doublet (middle-trace) is seen to split into five components (top trace) in an electric field. Three components labeled with the zero-field  $J$  value  $5/2$  have  $|M|$  values of  $1/2$ ,  $3/2$ ,  $5/2$ , and the two of  $J=3/2$  have  $|M|$  values of  $1/2$  and  $3/2$ . The frequency scale with markers every 125 MHz provided by transmission maxima from the etalon

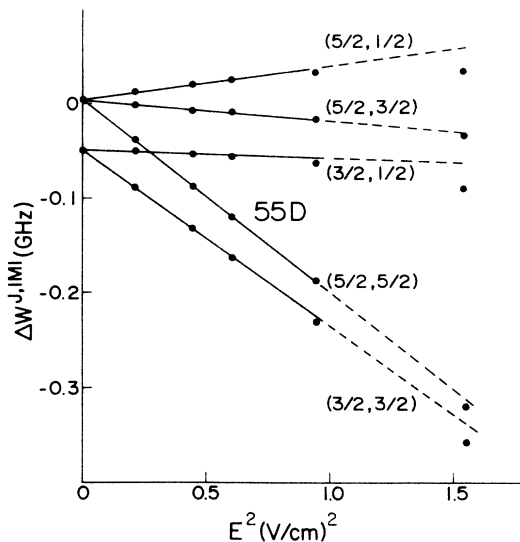


FIG. 3. Low-field Stark shifts of components  $J, |M|$  for the transition  $55^2D_{3/2,5/2} \leftarrow 5^2S_{F=3}$  plotted against  $E^2$ . Only the data from  $E=0$  to approximately 1.0 over which there is a quadratic dependence on  $E$  were used to evaluate the polarizabilities.

are displayed in the bottom trace. All of the observed Stark spectra exhibited linewidths of 4–20 MHz, due to pressure broadening, with the larger widths for states near  $n=20$  which have been shown to have higher rates of self-broadening.<sup>8</sup>

At a given electric field, the shift of each component

TABLE I. Scalar and tensor polarizabilities  $\alpha_0^J$  and  $\alpha_2^J$  of  $^2D$  states of Rb, in MHz/(V/cm)<sup>2</sup>, determined from measured Stark shifts and calculated using radial integrals given by Gounand.

$nD$	$\alpha_0^{5/2}(\text{obs})$	$\alpha_0^{5/2}(\text{calc})^a$	$\alpha_2^{5/2}(\text{obs})$	$\alpha_2^{5/2}(\text{calc})^a$
13	0.00704(6)	0.00757(36)	0.0047(1)	0.0047(3)
15	0.0198(1)	0.0199(10)	0.0151(2)	0.0154(8)
20	0.145(2)	0.143(9)	0.149(5)	0.151(7)
25	0.66(1)	0.65(5)	0.81(1)	0.84(4)
30	2.33(2)		3.2(1)	
35	6.3(2)		10.4(2)	
37	9.6(4)		15.3(4)	
40	16.7(4)		26.2(9)	
45	38(2)		64(3)	
50	72(4)		134(5)	
55	139(8)		254(10)	
$nD$	$\alpha_0^{3/2}(\text{obs})$	$\alpha_0^{3/2}(\text{calc})^a$	$\alpha_2^{3/2}(\text{obs})$	$\alpha_2^{3/2}(\text{calc})^a$
13	0.00781(3)	0.00801(34)	0.00269(6)	0.00285(14)
15	0.0214(2)	0.0213(11)	0.0088(2)	0.0094(4)
20	0.160(3)	0.155(9)	0.089(3)	0.094(4)
25	0.74(3)	0.71(5)	0.50(2)	0.52(3)
30	2.6(1)		1.95(5)	
35	7.4(2)		6.2(2)	
37	10.8(2)		9.2(3)	
40	18.5(7)		16.0(8)	
45	42(2)		39(3)	
50	85(3)		82(3)	
55	164(9)		163(10)	

<sup>a</sup>Errors quoted for the calculated polarizabilities are obtained by assuming a 0.5% error in the computed radial integrals from Ref. 5.

from its zero-field position was measured, and an average value was obtained from three or more spectral recordings. Measurements were corrected for thermal drift of the etalon ( $< 1$  MHz/min) by observing changes in the relative positions of etalon transmission maxima and reference cell spectra. For each  $J, M$  component, such Stark shift measurements were made for at least five different values of electric field. The field range for all components of a specific  $n^2D$  doublet was chosen to include fields over which the associated  $5/2, 5/2$  component shift was observed to depend quadratically on the field, as expected from Eq. (2). Graphs of Stark shift measurements versus  $E^2$  are presented in Figs. 2 and 3, for levels  $20^2D$  and  $55^2D$ . For level  $20^2D$ , the shifts of all five components vary as  $E^2$  over the field range shown, while for  $55^2D$ , the quadratic dependence only holds up to  $E = 1.0$  V/cm.

### V. ANALYSIS AND RESULTS

For a given  $^2D$  state, the measured Stark shifts of all five components were fitted simultaneously to Eqs. (2) using a least-squares fitting procedure. The sum of squares of differences between observed shifts and those calculated with Eqs. (2) were minimized by choosing optimum values of the four polarizabilities  $\alpha_0^{5/2}$ ,  $\alpha_2^{5/2}$ ,  $\alpha_0^{3/2}$ , and  $\alpha_2^{3/2}$ . The values of the scalar and tensor polarizabilities resulting from this analysis are listed in Table I. Quoted errors for these polarizabilities are twice the statistical errors determined with the fitting program. Also listed in this table are polarizabilities calculated with Eqs. (5) using computed radial integrals reported<sup>5</sup> for  $n \leq 28$ , and quantum defects determined from recent measurements.<sup>9,10</sup> The errors for these values were obtained by assuming relative errors of 0.5% in the computed radial integrals.

The experimental values of the polarizabilities were fitted to polynomials of the effective quantum number using a least-squares fitting program, in order to determine their  $n^*$  dependence. Both scalar and tensor polarizabilities corresponding to  $J = 5/2$  and  $3/2$  were best described by polynomials of the form given by Eq. (1), namely,  $\alpha_i = A_i(n^*)^7 + B_i(n^*)^6$  over the range of  $n = 13-55$ , or  $11.653 \leq n^* \leq 52.653$ . Coefficients of these polynomials are presented in Table II, along with the coefficients obtained from a similar analysis of polarizabilities calculated for  $n \leq 28$  using computed radial integrals.<sup>5</sup>

When the fine-structure spacings of intermediate  $^2P$  and  $^2F$  states are neglected in the energy denominators of Eqs.

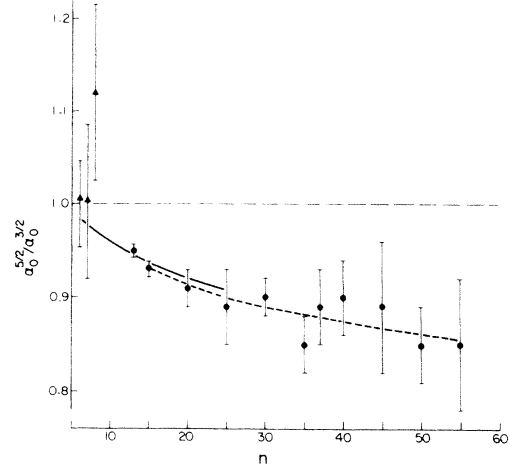


FIG. 4. Graph of the ratio  $\alpha_0^{5/2}/\alpha_0^{3/2}$  plotted against  $n$  for  $n^2D$  states of Rb. Included are the present data ( $\bullet$ ), those of Refs. 2, 3, and 4 for 6, 7,  $8^2D$  ( $\blacktriangle$ ), the calculated values based on radial integrals of Ref. 5 (solid line), and those based on the parameters in Table II (dashed line).

(5), the following identities are obtained for ratios of the scalar and tensor polarizabilities:

$$\alpha_0^{5/2}/\alpha_0^{3/2} = 1$$

and

$$\alpha_2^{3/2}/\alpha_2^{5/2} = 7/10. \quad (6)$$

For excited  $D$  states of Rb these relations are only approximate as the fine-structure splittings of intermediate  $^2P$  states lead to significantly lower values of the ratios which vary slowly with  $n$ . Graphs of these ratios versus  $n$  display their monotonic variations (Figs. 4 and 5). At high  $n$ , the ratios tend towards constant values of 0.78(4) and 0.62(2), for the scalar and tensor polarizabilities, respectively. This behavior is expected since the  $n$  dependence of the energy denominators in Eqs. (5) is the same as that of the fine-structure spacings of the highly excited intermediate states, namely,  $\Delta_{FS} \sim n^{-3}$ . Thus, even though the fine-structure spacings become negligible at high  $n$ , their contributions to the energy denominators remain significant. Included in Figs. 4 and 5 are ratios resulting from the present measurements, and from those of Svanberg and co-workers,<sup>2-4</sup> as well as ratios calculated using the computed radial integrals of Gounand.<sup>5</sup>

TABLE II. Coefficients  $A$  and  $B$  of Eq. (1) for  $n^*$  scaling of polarizabilities, obtained from the present measurements, and when data for 6– $8^2D$  (Refs. 2–4) are included, as well as values calculated using computed radial integrals given in Ref. 5.

	$\alpha_0^{5/2}$	$\alpha_2^{5/2}$	$\alpha_0^{3/2}$	$\alpha_2^{3/2}$
$(n^*)^7$ coefft. (present)	$7.2(3) \times 10^{-11}$	$2.28(5) \times 10^{-10}$	$9.1(2) \times 10^{-11}$	$1.42(4) \times 10^{-10}$
(calc.)	$6(1) \times 10^{-11}$	$2.4(1) \times 10^{-10}$	$7(1) \times 10^{-11}$	$1.54(5) \times 10^{-10}$
(incl. 6– $8^2D$ )		$2.27(3) \times 10^{-10}$		$1.4803(5) \times 10^{-10}$
$(n^*)^6$ coefft. (present)	$2.09(2) \times 10^{-9}$	$-7.7(9) \times 10^{-10}$	$2.06(4) \times 10^{-9}$	$-5.7(6) \times 10^{-10}$
(calc.)	$2.34(15) \times 10^{-9}$	$-9.6(1.5) \times 10^{-10}$	$2.32(16) \times 10^{-9}$	$-6.6(6) \times 10^{-10}$
(incl. 6– $8^2D$ )		$-6.6(2) \times 10^{-10}$		$-5.7(6) \times 10^{-10}$
$(n^*)^5$ coefft. (incl. 6– $8^2D$ )		$-1.45(8) \times 10^{-10}$		

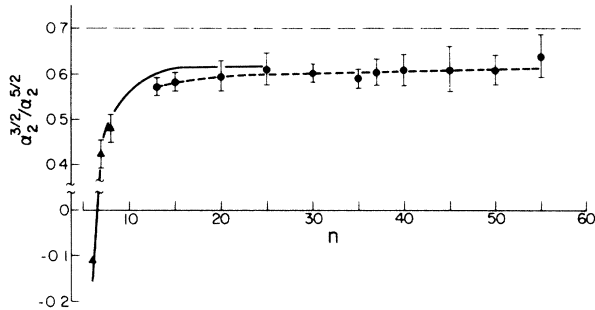


FIG. 5. Graph of the ratio  $\alpha_2^{3/2}/\alpha_2^{5/2}$  plotted against  $n$  for  $n^2D$  states of Rb. Included are the present data ( $\bullet$ ), those of Refs. 2, 3, and 4 for 6, 7,  $8^2D$  ( $\blacktriangle$ ), the calculated values based on radial integrals of Ref. 5 (solid line), and those based on the parameters in Table II (dashed line).

These results show that scalar and tensor polarizabilities of Rb  $^2D$  states (either for  $J=3/2$  or  $5/2$ ) are not linearly related owing to the  $^2P$ -state fine-structure splitting. Furthermore, Eqs. (5) can be truncated to include only neighboring intermediate states. It follows from inspection of Eqs. (5) that, in principle, radial integrals corresponding to transitions from  $n^2D$  to  $(n+1)^2P$  and  $n^2D$  to  $(n+2)^2P$  states can be deduced from the four polarizabilities associated with each  $n^2D$  level. However, the experimental errors of the present polarizabilities were such as to permit only the estimate of integrals for the  $n^2D$  to  $(n+1)^2P$  transitions. These values are listed in Table III along with values computed by Gouand.<sup>5</sup>

Intensity measurements of the five  $^2D$  components were made for several of the observed spectra recorded at low fields (i.e., with  $\Delta_{FS} > \Delta W^{J,|M|}$ ) using laser light polarized at  $45^\circ$  to the electric field. For the  $35^2D_{3/2,5/2} \leftarrow 5^2S_{F=3}$  transitions, the average peak intensities at five different fields for the components  $J, |M|$ , namely,  $(5/2, 5/2):(5/2, 3/2):(5/2, 1/2):(3/2, 3/2):(3/2, 1/2)$  were found to be 27(3):109(10):46(5):32(3):71(7). These results are in fair agreement with the values 31:100:65:36:62 calculated from the theory of two-photon absorption which neglects Stark mixing between states of the fine-structure doublet.<sup>11</sup>

## VI. DISCUSSION

The only other evaluations of  $^2D$  state polarizabilities of Rb were those made by Svanberg and co-workers<sup>2-4</sup> for 6,

TABLE III. Comparison of radial integrals for  $n^2D \leftrightarrow (n+1)^2P$  transitions derived from measured polarizabilities and calculated values reported in Ref. 5.

$n^2D \leftrightarrow (n+1)^2P$		$\alpha_0^{-1} R_{(n+1)^2P}^{n^2D}$	
		obs.	calc. <sup>a</sup>
13	14	194(50)	183
15	16	274(75)	252
20	21	520(150)	472
25	26	800(300)	759
30	31	1200(400)	
35	36	1800(650)	
37	38	1800(800)	
40	41	2100(850)	
45	46	2700(1900)	
50	51	3500(1900)	
55	56	3800(2300)	

<sup>a</sup>Calculated values available for  $n$  up to 28.

7, and  $8^2D$ . Their values are compared in Table IV with predicted values obtained by extrapolating the  $n^*$ -scaling equations which resulted from measurements of the present work. It is seen that there is good agreement between predicted and measured scalar polarizabilities (with the predicted values being three times more precise than the earlier experimental values).

The predicted tensor polarizabilities are less precise, however, because of a near cancellation of  $(n^*)^6$  and  $(n^*)^7$  terms in the  $n^*$ -scaling equations close to  $n=6$ , which makes the predicted values very sensitive to even small errors in the  $A$  and  $B$  coefficients of Eq. (1). With this qualification, there is general agreement between predicted tensor polarizabilities and the values reported in Refs. 2-4. The precision of the  $n^*$ -scaling coefficients for tensor polarizabilities was improved by including the measurements of Refs. 2-4 in the analysis, and the new coefficients are given in Table II. The resulting improvement is most striking for  $\alpha_2^{3/2}$  while an additional term ( $n^{*5}$ ) was necessary to describe the dependence of  $\alpha_2^{5/2}$ . These results are expected since the polarizabilities of low-lying excited states give information regarding lower power terms in the  $n^*$ -scaling equations which can be written in the following general form:

$$\alpha = \sum_{k=0}^{\infty} A_k (n^*)^{(7-k)}.$$

TABLE IV. Comparison of scalar and tensor polarizabilities  $\alpha_0^J$  and  $\alpha_2^J$ , for  $^2D$  states of Rb, in  $\text{MHz}/(\text{V}/\text{cm})^2$  reported in Refs. 2-4, and values based on the present measurements.

Level	$\alpha_0^J$		$\alpha_2^J$	
	Refs. 2-4	Present	Refs. 2-4	Present
$6^2D_{3/2}$	$2.5(1) \times 10^{-5}$	$2.63(5) \times 10^{-5}$	$-1.05(7) \times 10^{-7}$	$10(9) \times 10^{-7}$
$7^2D_{3/2}$	$8.4(6) \times 10^{-5}$	$8.6(2) \times 10^{-5}$	$5.0(3) \times 10^{-6}$	$8(3) \times 10^{-6}$
$8^2D_{3/2}$	$2.1(2) \times 10^{-5}$	$2.34(5) \times 10^{-4}$	$2.7(1) \times 10^{-5}$	$3(1) \times 10^{-5}$
$6^2D_{5/2}$	$2.4(1) \times 10^{-5}$	$2.57(3) \times 10^{-5}$	$9.4(5) \times 10^{-7}$	$2(2) \times 10^{-5}$
$7^2D_{5/2}$	$8.5(3) \times 10^{-5}$	$8.3(1) \times 10^{-5}$	$1.17(5) \times 10^{-5}$	$7(6) \times 10^{-5}$
$8^2D_{5/2}$	$2.4(1) \times 10^{-4}$	$2.26(3) \times 10^{-4}$	$5.6(3) \times 10^{-5}$	$2.0(1.4) \times 10^{-4}$
$9^2D_{5/2}$			$1.8(9) \times 10^{-4}$	$5(4) \times 10^{-4}$

Measured polarizabilities and their associated  $n^*$ -scaling coefficients are in reasonable agreement with calculations based on computed radial integrals. The observed differences between measured and calculated values are consistent with an assumed uncertainty of  $\sim 0.5\%$  in the computed integrals.<sup>5</sup> Radial integrals of  $n^2D$  to  $(n+1)^2P$  transitions for  $13 \leq n \leq 55$  deduced from the present measurements, also agree with the values for  $n \leq 28$ , computed by Gounand.<sup>5</sup>

## VII. CONCLUSIONS

The scalar and tensor polarizabilities of excited  $n^2D$  states of Rb over the range  $n = 13-55$  have been determined for the first time, their accuracies being 1–10%. The derived values were found to depend on the effective quantum numbers according to relations of the form  $\alpha = A(n^*)^7 + B(n^*)^6$ . Values of polarizabilities obtained by extrapolation to low  $n^*$  agreed with the only existing

values, those for 6, 7, and  $8^2D$  levels, measured by Svanberg and co-workers. Polarizabilities calculated from computed radial integrals were in reasonable agreement with the values obtained here, and integrals derived for  $n^2D \leftrightarrow (n+1)^2P$  transitions agreed with the available values up to an  $n=28$  computed by Gounand.

## ACKNOWLEDGMENTS

We wish to thank S. Svanberg for permission to use and to make reference to unpublished results, and K. A. H. van Leeuwen for helpful discussions and for providing a copy of his thesis. This research was supported in part by the Natural Sciences and Engineering Research Council of Canada (NSERC) and the University of Toronto. One of us (M.S.O.) is grateful to NSERC and the University of Toronto for financial support during the course of this research.

---

\*Present address: Northern Telecom Canada Ltd., 8 Colonade Rd., Nepean, Ontario, Canada K2E 7M6.

<sup>1</sup>M. S. O'Sullivan and B. P. Stoicheff, *Phys. Rev. A* **31**, 2718 (1985).

<sup>2</sup>W. Hogervorst and S. Svanberg, *Phys. Scr.* **12**, 67 (1975).

<sup>3</sup>K. Fredriksson and S. Svanberg, *Z. Phys. A* **281**, 189 (1977).

<sup>4</sup>F. Fredriksson, L. Nilsson, and S. Svanberg (unpublished).

<sup>5</sup>F. Gounand, *J. Phys. Paris* **40**, 457 (1979).

<sup>6</sup>A. Khadjavi, A. Lurio, and A. Happer, *Phys. Rev.* **167**, 128 (1968); K. A. H. van Leeuwen, Ph.D. thesis, *Natuurkundig*

*Laboratorium der Vrije Universiteit, The Netherlands*, 1984.

<sup>7</sup>M. S. O'Sullivan, Ph.D. Thesis, University of Toronto, Canada, 1985.

<sup>8</sup>B. P. Stoicheff and E. Weinberger, *Phys. Rev. Lett.* **44**, 733 (1980).

<sup>9</sup>B. P. Stoicheff and E. Weinberger, *Can. J. Phys.* **57**, 214 (1979).

<sup>10</sup>C.-J. Lorenzen and K. Niemax, *Phys. Scr.* **27**, 300 (1983).

<sup>11</sup>G. Grynberg and B. Cagnac, *Rep. Prog. Phys.* **40**, 791 (1977), and quoted references.